# Chapter I

# Introduction

*"Man needs difficulties in life because they are necessary to enjoy the success."*

*-A.P.J Abdul Kalam*

## 1.1 Background

In Greek, nano means dwarf. Literally, nano signifies to the one billionth or $10^{-9}$ power. Nanoscience is an interdisciplinary concept where different branches of science, such as, physics, chemistry, biology, engineering etc. are suitably involved. Nanoscience and nanotechnology deals with the capability to produce, characterize and manipulate artificial structures that are well-regulated at the nanoscale level. In fact, nanoscale structures (1-100 nm) already existed in the nature before scientists artificially synthesized in the laboratories. The building block of all living entities basically represent a single strand of deoxyribonucleic acid (DNA), is about ~ 2.5 nm wide [1].

Though the curiosity behind studying nanometric systems has become a subject of scientific interest, the perception was actually originated centuries ago. The concept of nanoscience was first penned by the physicist Richard Feynman in 1959, in his revolutionary lecture "*There's plenty of room at the bottom*" in the annual meeting of the American Physical Society held at the California Institute of Technology [1]. Feynman introduced the prospective manipulation of material at the nanoscale level [1]. The term 'nanotechnology' was first used by the Japanese scientist Prof. Norio Taniguchi. He in an international conference on Production Engineering held at Tokyo in 1974 discussed the capability to engineer materials, specifically at the nanoscale level. The development of sophisticated tools has significantly influenced and strengthened our understanding of the nanoscale world. A key step in this track was the invention of the scanning tunneling microscope (STM) in 1982, and the atomic force microscope (AFM) in 1986. These sophisticated tools are capable of imaging a surface with atomic resolution, and also have ability to picking up, sliding or dragging atoms or molecules around on surfaces of the nanosytems.

The modern microscopic systems and tools have offered the potential to collect figures associated to structural details and surface phenomena.

The properties of nanomaterials are significantly different from their bulk counterpart. When the dimension of a material is reduced below 100 nm, dramatic changes occur as regard physical properties. Based on the nature of quantum confinement, different kinds of low dimensional structures have been observed. If the confinement is specifically along one direction, the structure is known as a two dimensional (*2D*) quantum well. If confinement is along two directions, the structure is referred as a one dimensional (*1D*) quantum wire. In contrast, a quantum dot is a system where carrier motion is confined in all the three dimensions. All these structures are subjected to quantum-mechanical rules. Figure 1.1 represents the density of states for *3D, 2D, 1D* and *0D* quantum systems.

The applications of different nanoscale materials have found its importance in day- to- day life as well as in industry. The several scientific and research areas in which these materials have found profound interest includes electronics, energy, biology, medical technology, information and communication technology etc. For instance, nanomaterials can be extremely useful in the making of sunscreen lotions, durable paints, antioxidants, food processing, electromagnetic (EM) shielding etc. [2-4]. The solar cells, high performance batteries, capacitors, and hydrogen storage devices have already been examined [5-8].

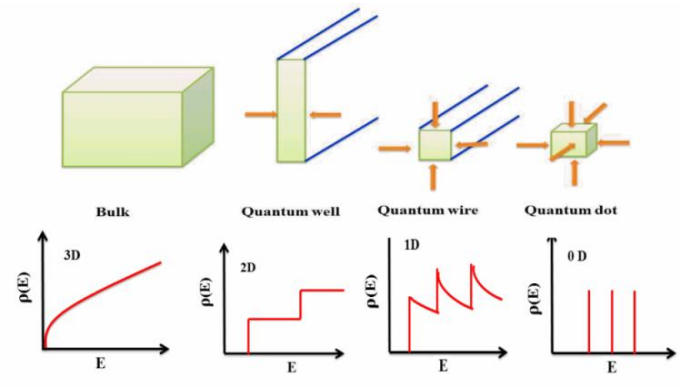


Figure 1.1: Schematic diagrams of density of states vs. energy for *3D, 2D, 1D* and *0D* systems.

In the field of bio-medical engineering, nanomaterials have numerous opportunities as regards diagnostics and therapeutics perspectives. Nanosytems are trained in such a way that they can help direct treatment of unhealthy cells [9]. Moreover, their immense value has been realized in designing field emission devices [10]. This thesis is basically focused on rare earth $Gd_2O_3$ and $Gd_3O_4F_6$ based nanostructured systems.

### 1.2 Rare earth oxide (REO) based nanostructures

In the periodic table, rare earth elements are recognized as *f*-block elements which comprise of two series: lanthanide and actinide series. A part of the lanthanide series elements are shown in Figure 1.2. Almost all RE elements are non-radioactive metals and their oxides are normally found in the form of monoxides (REO), sesquioxides ($RE_2O_3$) and dioxides ($REO_2$). The sesquioxide form is thermally, chemically and environmentally stable as compared to than other oxides. In general, RE materials adopt a stable trivalent ($RE^{3+}$) state, though other oxidation states ($RE^{2+}$), ($RE^{4+}$) are also possible. Sm, Eu and Yb can exhibit both +2 and +3 oxidation states. Ce is the only RE element that can exist in $Ce^{4+}$ form [11].

In recent time, the RE oxide based nanosystems have gained increased scientific and industrial interest. Pure RE systems, or their oxides, have immense potential in imaging, optoelectronic and biomedical applications as they exhibit remarkable magnetic and optical properties [12]. The luminescent properties of the RE elements are found to be extremely useful for fabricating devices, such as, plasma panels, flat panel displays, luminescent lighting, infra-red (IR) windows, etc. [13,14]. The RE elements are unique in the sense that, the *f*-shell containing unpaired electrons is interlocked unlike transition metal elements. Subject to the selection rules, the luminescence is caused through definite *D-F* transitions. The RE materials though known for its rarity, however, environmental and chemically stability and durability make them highly promising assets in modern technology.

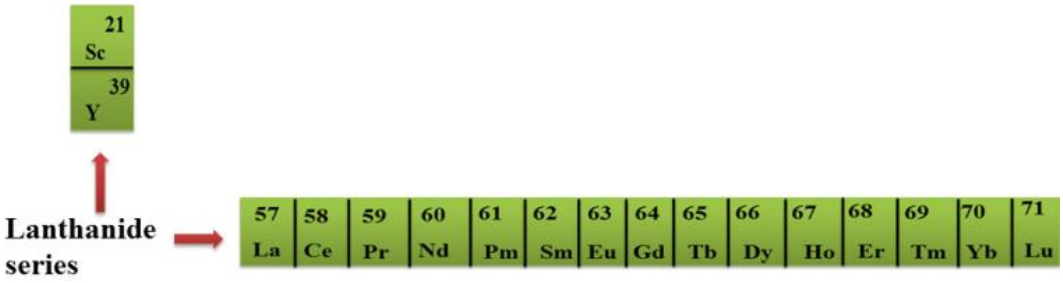


Figure 1.2: Part of the modern periodic table (lanthanide series)

The REO exhibited different crystallographic structures as illustrated by their phase diagram (Figure 1.3) [15, 16]. In ambient environment, the hexagonal (*A*) phase exists for large ionic radius (La↔Nd). The *A* phase, whose cations are in the seven-fold coordination, has space group *P-3m1* and contains one molecule per unit cell. The cubic *C*-form occurs for smaller RE cations (Tb↔Lu). The *C*-phase, whose cations are in six-fold coordination, has a cubic structure with the space group *Ia-3* and possessing 16 molecules per unit cell [17]. The intermediary RE elements (Sm↔Gd) can be obtained either in the cubic (*C*) or in the monoclinic (*B*) form. The *B* phase, whose cations are mixed with six or sevenfold coordination, has a monoclinic structure with the space group *C2/m* having six molecules per unit cell [17]. At high temperature (2300–2500 K), hexagonal, monoclinic and cubic (*A*, *B*, and *C*) phases get converted to the hexagonal H-form ($P6_3/mmc$). The cubic *X* phase form with space group $1m\bar{3}m$, at moderately high temperatures (2400–2700 K) for compositions with cations larger than that of Dy. The crystal structures of the three different polymorphs of RE sesquioxides ($RE_2O_3$) are depicted in Figure1. 4.

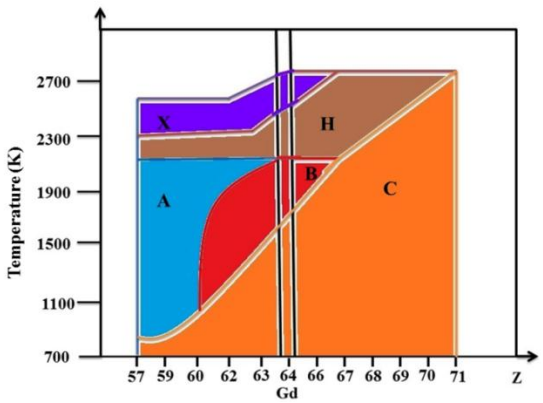


Figure 1.3: Phase diagram of rare earth sesquioxides ($RE_2O_3$) [15].

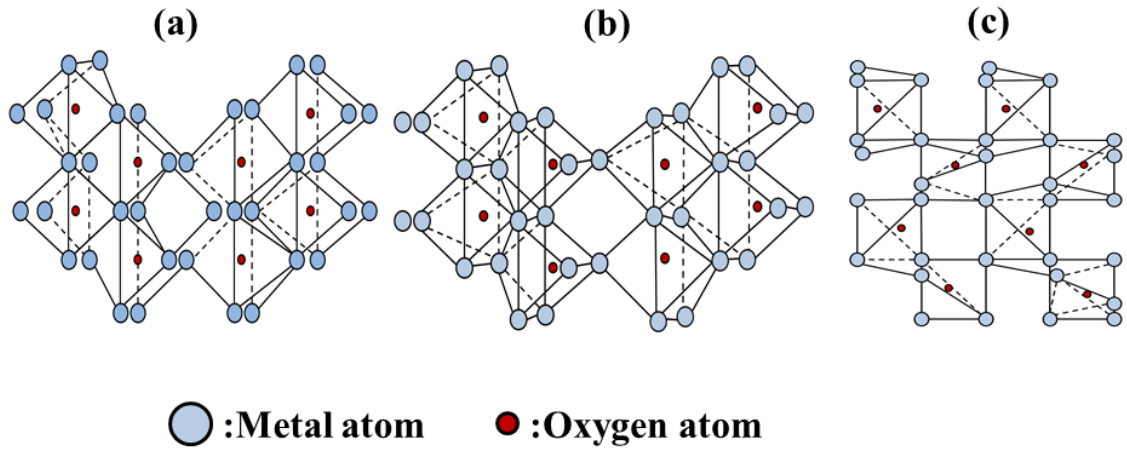


Figure 1.4: Different crystal structure of $RE_2O_3$: (a) hexagonal (b) monoclinic and (c) cubic

The trivalents ($RE^{3+}$) are capable of exhibiting strong and sharp emission peaks in or near the visible region of the electromagnetic spectrum. The energy levels of these ions are discrete in nature. This is due to the strong shielding provided by *6s* and *5p* electrons to the *4f* electrons, which are less affected by the crystallographic environment. Consequently, the RE sesquioxide ($RE_2O_3$) containing the $RE^{3+}$ ions display sharp emission, responses which is quite typical of those ions. The $RE^{3+}$ ions offer wide range of emission colours and are extremely stable, against environment.

Nanoscale magnetic and luminescent materials are attractive in the field of nanobiotechnology as their dimension is comparable to biological structures such as DNA (2.5 nm), proteins (5 nm), and antibodies (10 nm) [1]. For analytical, diagnostic, and therapeutic purposes, these nanoscale systems can be used at large [18]. While luminescent nanosystems find application as tags particularly in bio-imaging, magnetic nanosystems are employed for tracking organelles or small molecules in cells, tissue repair, drug delivery, magnetic resonance imaging, etc. [19]. In recent years, semiconductor quantum dots have been extensively used for a wide variety of biological applications. In spite of bright emission, however, these QDs suffer from several issues. The QDs which are composed of heavy metals may cause toxicity in the system, when available as free species. On the other hand, RE oxide based nanosystems are

more stable both chemically and environmentally, and thus become less toxic. As compared to organic dyes, the RE systems are found to offer superior role in tagging and bio-labeling applications.

Usually, it is difficult to synthesize REO based nano dimensional systems following a direct top-down method. This is because, a REO is highly stable which possess high thermal, chemical and mechanical stability. Nevertheless, the bottom-up method is rather easy. Earlier, a number of researchers considered physico-chemical routes to synthesize nano-sized REOs. For instance, sol-gel method [20], hydrothermal route [21-23], combustion synthesis [24,25], sono-chemical route [26,27], emulsion and microemulsion route [28], precipitation method [29], chemical vapour deposition [30, 31] methods have been employed. The morphology and shape of nanoparticles are also shown to be controlled via the use of surfactants or capping agents [32-34]. Previously, nano ceria ($CeO_2$) was fabricated by using different surfactants, like, sodium dodecyl sulfate (SDS), polyethylene glycol (PEG), cetyl trimethylammonium bromide (CTAB) etc. [35]. Similarly, yttrium oxide ($Y_2O_3$) based nanosystem has also been prepared via gas condensation route [36].

One dimensional (1D) nanostructured systems, such as, nanorods, nanotubes, nanowires have shown their immense potential in various fields due to their outstanding shape-specific quantum confinement effect. Du et al. have reported the synthesis of 1D gadolinium hydroxide ($Gd(OH)_3$) nanosystems by employing a simple hydrothermal treatment [37]. Cao et al. have reported the fabrication of 2D $Gd_2O_3$ nanoplates using a decomposition route [38]. Using a similar synthetic route, 2D $Pr_2O_3$ nanoplates and $Eu_2O_3$ nanodisks are produced by other groups [39]. On the other hand, synthesis of REO nanotubes has also become possible [40]. Figure1.5 represents some of the fascinating electron microscopic images of different RE based nanoscale systems.

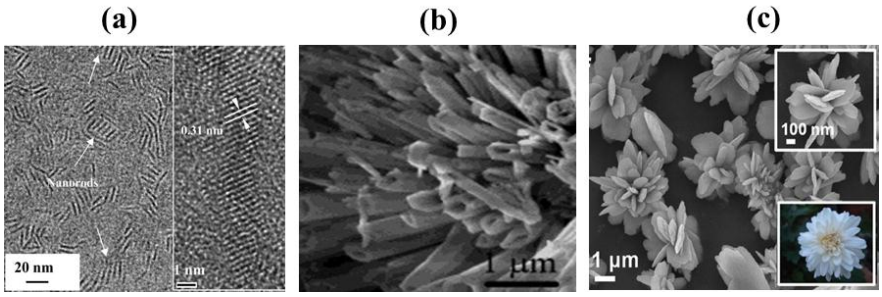


Figure 1. 5: (a) HRTEM image of $Gd_2O_3$ nanorods [41] (b) SEM image of $Dy_2O_3$ nanotubes [42] (c) SEM image of $Gd_2O(CO_3)_2 \cdot H_2O$ nanoflowers [43].

### 1.3 Rare earth oxyfluoride systems

Different inorganic nanomaterials, such as, RE oxides and fluorides owing to their matchless chemical and thermal stability are regarded as excellent host for down and upconversion luminescence response [44]. In general, the controlled dispersion of the optically active RE materials in appropriate host matrices becomes crucial for providing a confined environment in which the luminescent centres could influence the light-emission characteristics, to a great extent. The radiative decay of the RE the ions may suffer from quenching effects in the case of RE clustering and /or vibronic coupling within the host matrix [45].

The nano-dimensional RE doped lanthanide oxide and lanthanide fluorides are highly demanding in the area of biomedical engineering field as they have both fluorescence and magnetic properties. The collective property can have potential in magnetic resonance imaging (MRI), labelling and drug-release/loading owing to their high surface area and low density [46]. Due to their exceptional chemical bonding between metal cations and fluoride anions, lanthanide fluoride nanospheres have received numerous attention over oxide systems [47-50].

The crystallographic properties of RE oxyfluoride (REOF) have been worked out by Zachariasen et al. in early 1950s [51]. It has been confirmed that a solid state reaction between RE fluorides and their oxides at high temperatures, could form oxyfluorides [52]. Normally, REOFs appear in two phase such as

tetragonal and rhombohedral [51]. The variation of tetragonal phase is due to high similarity of ionic radius between $F^-$ and $O^{2-}$. These ions can exchange each other in the crystal structure owing to similar ionic radii. In addition to tetragonal and rhombohedral phases, cubic phase of the REOF can also exist [53, 54]. The space groups allocated to tetragonal *P4/nmm* and rhombohedral $R\bar{3}m$. For tetragonal phase, $RE^{3+}$ ions occupy sites with $C_{4v}$ symmetry while in the rhombohedral structure, the local symmetry of $RE^{3+}$ is $C_{3v}$ [55]. The structure of gadolinium oxyfluoride GOF ($Gd_3O_4F_6$) and unit cell geometry are shown in schematic Figure 1. 6.

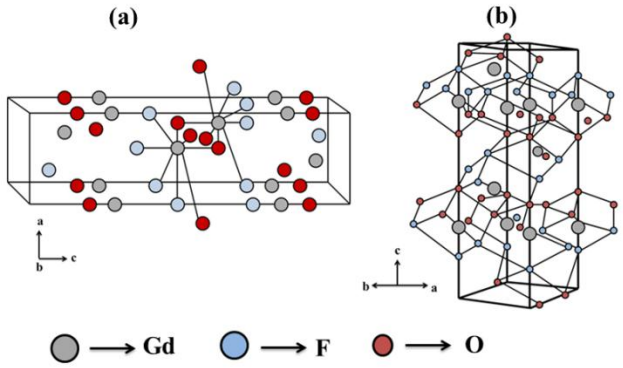


Figure 1.6: Structure of gadolinium oxyfluoride ($Gd_3O_4F_6$) (a) tetragonal [56] and (b) rhombohedral [57] forms.

Figure 1.7 depicts RE oxyfluoride based nanosytems with different morphologies.

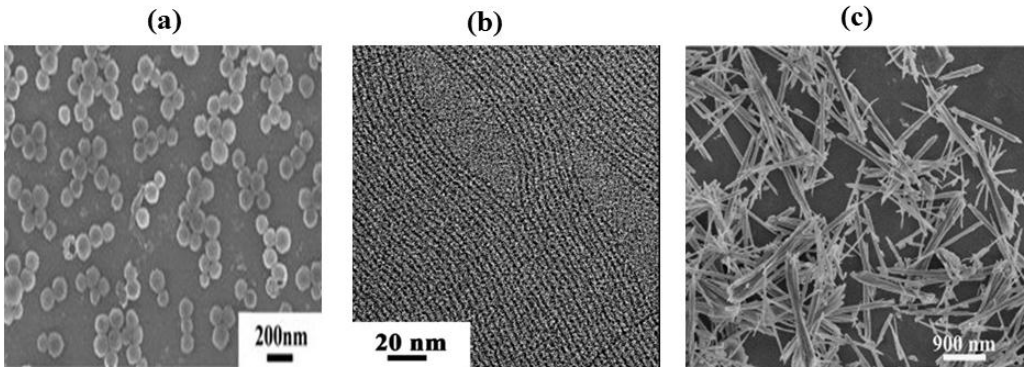


Figure1.7: Electron microscopy images of different RE oxyfluorides (a) GOF nanospheres [44], (b) EuOF nanowires [47] and (c) GOF nanorods [56].

## 1.4 Properties of RE oxides and oxyfluoride based nanoscale systems

The RE nanosytems are recognized for their outstanding optical and optoelectronic properties. Not surprisingly, superb white light can be obtained on combining three monochromatic sources (red, green and blue) and when RE systems are mixed in appropriate quantities. Gadolinium oxide ($Gd_2O_3$) is a well-known host for the selective luminescence response of many RE ions [58, 59]. Normally, $Eu^{3+}$ and $Tb^{3+}$ ions act as active luminescent centers in display components/elements [60]. It is worth mentioning here that, apart from there $Tb^{3+}$, $Dy^{3+}$, and $Eu^{3+}$ ion doped $Gd_2O_3$ nanosytems have also desired application in optoelectronic industry, immunoassays etc.[61]. The host $Gd_2O_3$ has a strong absorption around 230–240 nm and exciting the host could facilitate energy transfer between the host and the luminescent ions [62]. Owing to $4f$–$4f$ or $5d$–$4f$ transitions, the RE ions exhibit diverse emission colours. Some of the RE ions such as, $Eu^{3+}$ , $Tb^{3+}$, $Dy^{3+}$ display strong red/orange (611nm /590 nm), green (544 nm) , blue (460–505 nm) and yellow (570–600 nm) emissions respectively.

The RE oxides have wide range of band gaps between 3.0-6.0 eV [63]. Due to $4f^n$ configuration of the $Ln^{3+}$ ions wide band gaps occurred. The dielectric constant ($\epsilon_r$=7-20) and electrical resistivity ($\rho=10^{12}$-$10^{15}$ Ω cm) of these oxides are also reasonably high [64, 65]. The $Ln^{3+}$ ions have the capability to emit visible or UV light following an excitation with low energy near infrared (NIR) radiation mediated via a multiphoton process known as upconversion [62]. The doping of $Yb^{3+}$ illustrates a green and red upconversion of $Gd_2O_3$: Er+Yb samples [66]. In solar cell application lanthanide ion doped nanomaterials are also extensively used [67].

On the other hand, RE oxyfluorides are regarded as excellent host materials due to their high transparency, low phonon energy and higher probability of nonradiative transitions associated with the $Ln^{3+}$ ions [68, 69]. Lanthanide oxyfluorides (LaOF) at nanoscale level exhibited notable up and downconversion photoluminescence (PL) responses [45, 70, and 71]. It was

observed that the $Eu^{3+}$, $Yb^{3+}/Eu^{3+}$ and $Tm^{3+}/Ho^{3+}$ doped LaOF materials would give rise to intense red, green, and blue emission upon irradiation from the UV to NIR regions [72–74]. It may be noted that, trigonal LaOF can show multi-color tunable emission properties when doped with Eu, Tb, Sm, Dy, Tm, and/or Ho thereby ensuring their potential use in the field emission display devices [75,76]. Furthermore, GOF systems, (tetragonal and trigonal) have been employed for white light upconversion due to codoping of Er/Tm/Yb [57,77,78].

### 1.5 Effect of swift heavy ion irradiation on nanomaterials

Ion irradiation is a nifty technique that is capable of manifesting structural and morphological properties of matter in a controlled manner. When an energetic ion traverses through a solid, two distinctly different types of collisions occur with the target atoms [79]. This encounter implies energy transfer from the projectile ion to the target material. The energetic ions deliver energy through different energy loss mechanisms: nuclear ($S_n$) and electronic ($S_e$) collision [79, 80]. The interaction between ion and matter is schematically presented in Figure 1.8 [79].

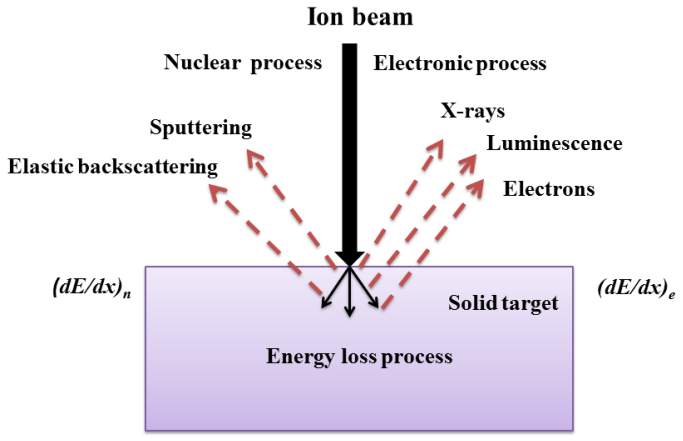


Figure 1.8: Schematic of different events during ion matter interaction process

In the nuclear collision process, the collisions between the incident ions and lattice atoms, where conservation of energy and momentum is relevant is regarded as, elastic process. During nuclear collisions, the incident ion scatter

back from the surface of the material elastically, which results in the ejection of target atoms from the surface or may come into rest after migrating a few atomic spacing underneath the surface [79]. Alternatively, the electronic collision process is involved with the interaction of fast ions and with the lattice electrons. This implies the emission of X-rays, Auger and secondary electrons [79]. Now the net energy loss over a depth $x$, is the sum of the nuclear and electronic energy losses and given by :

$$S=S_n + S_e$$

$$\text{or,} \qquad \frac{dE}{dx} = \left(\frac{dE}{dx}\right)_n + \left(\frac{dE}{dx}\right)_e \ , \qquad (1.1)$$

where, $S_n$ and $S_e$ signify the nuclear and electronic energy losses [81]. For ions with energy in the orders of several keVs, the nuclear energy loss ($S_n$) is dominant over electronic energy loss ($S_e$). Therefore, atomic displacements through elastic collisions would occur in the keV regime. Due to the displacement of atoms, numerous point defects can be expected [82, 83]. The projectile ion, after a series of collisions loses its energy steadily and finally comes to rest at a finite distance from the surface of the target, called as the projectile range ($R_p$). The projectile range ($R_p$), in case of keV scale irradiation, is always smaller than the sample dimension to facilitate implantation along the incident direction of the ions [79].

On the other hand, the electronic energy loss is believed to be caused by the inelastic collision of incident ions with the atoms of the target material and becomes dominant in the MeV scale of energy regime (typically >1 MeV/nucleon). In MeV irradiation, owing to high energy deposition, within a very short span of time, columnar tracks of the molten zone are generally formed along the ion trajectories [84]. The creation of the latent tracks is described by two competitive models: Coulomb explosion model and the thermal spike model [81]. In the Coulomb explosion, the electrostatic repulsion between the ions produced in the wake of the incident ion can be solely responsible for completely disordered/amorphized destruct the lattice [81, 84].

On the other hand, thermal spike model is the consequence of electronic excitation by the energetic ions, with energy transferred ultimately as heat to the lattice atoms by virtue of electron-phonon interaction. This implies an enormous increase of local lattice temperature, which is well above the melting point of the system. The increase in temperature is followed by rapid quenching and consequently, amorphized latent tracks in the system are formed [85-87].

By and large, the energy deposition leads to a noteworthy change of physical characteristics of the target material [88-90]. As far as oxide nanostructured systems are concerned, numerous reports are available in the literature which highlight irradiation induced modification of structural and optical responses [91,92]. The bombardment of energetic ions leads to change in the structural and morphological features, like particle growth [93], elongation [94], ripple formation [95], phase change [96], etc. In MeV scale, the nanoparticle growth, and nanoparticle splitting have been reported, whereas ion implantation and ripple formations are witnessed for on KeV scale irradiation [93,95]. On the other hand, the impact of ion irradiation has also been analyzed for stable RE sesquioxides [96-98]. Earlier Tang and co-workers have studied phase transformation (from cubic to monoclinic) aspects in $Dy_2O_3$ and $Er_2O_3$ systems and by using low energy ion irradiation (300 keV $Kr^{++}$) [96]. The ions are believed to produce dense displacement cascades in the target material. Due to excessively high temperature in the thermal spike, the specimen recrystallizes into a high temperature crystalline phase. On rapidly quenching the thermal spike, the high temperature metastable phase gets transformed into a stable monoclinic phase. As a second proposition, swift heavy ion (SHI) provides significantly high thermal activation energy for atomic displacement. Accordingly, defects can be induced at large. The enhancement of free energy as a result of ion-induced accumulation of defects can also be considered as the prime cause of phase transformation. A manifested, overall free energy of the irradiated samples can be dominant over the equilibrium phase (cubic phase) and that, monoclinic phase is likely to form upon recrystallization [96]. On the

other hand, the Coulomb explosion model can also justify phase transformation aspect through a different mechanism. It is based on the charge separation between the sputtered electrons and the transiently ionized atoms followed by violent repulsion between the ionized species. This ionic repulsion can then lead either directly to atom displacements or to the propagation of a shock wave, thereby inducing a transition of phase [89,99]. The fragmentation of rod-shaped ZnO nanostructures into spherical nanoparticles has been observed as a result of SHI impact [92]. Owing to excellent thermal and mechanical stability of the gadolinium oxides, the morphology evolution and shape alteration at the surface may have great impact when subjected to MeV scale energetic irradiation.

### 1.6 Principles of rheology and scope of non-Newtonian fluids

Rheology characterize the flow property of matter. It deals with the flow and deformation of matter when subjected to an external force. The term 'rheology' is derived from a Greek word "rheos" which means to flow. The word rheology was first coined by Eugene C. Bingham in 1920.

According to Newton's law of viscosity, the shear stress ($G$) is directly proportional to the shear rate ($\dot{\gamma}$) [100]:

i.e. $$G = \eta_v \dot{\gamma} \qquad (1.2)$$

The proportionality constant ($\eta_v$) is entitled as the viscosity of the system. Consequently, the rate of deformation under the applied stress is constant in a Newtonian liquid, which regains its shape and structure, once the stress is withdrawn. In fact, the Newtonian behavior gives a linear relationship between the shear stress and the shear rate. If shear- stress vs. shear-rate gives a nonlinear trend, it is called as a non-Newtonian fluid. Among non-Newtonian characteristics, the most studied system is "shear thinning" one which depicts a reduction in viscosity with increasing shear rates. On the other hand, if viscosity increases with increase in share rate, then it is called "shear thickening" property. The viscoplastic materials display a yield stress. When a

small amount of stress is applied, the material behaves like a solid and then flows with a constant differential viscosity for higher shear stresses. In this case, it is called as Bingham plastic material [100]. We can write,

$$G = G_0 + \eta_v \dot{\gamma} \quad (1.3)$$

where $G$ is shear stress, $G_o$ is yield stress, $\eta_v$ is viscosity and $\dot{\gamma}$ is shear rate. Certain food items display this kind of behavior.

If the viscosity of materials decreases with time of constant shear it is called "thixotropic". Alternatively, in rheopectic liquid, the viscosity is increased over time at a constant shear rate. Once the shear stress is removed, the apparent viscosity gradually decreases and returns to its original value [100].

It is worth mentioning here that, the entirely rheological behavior, whether time dependent or related to changes in shear, is influenced by the changes in the microstructure of the system. The flow curves related to Newtonian and non-Newtonian types are shown in Figure 1.9. There exist models to define the shear thinning behavior as a function of the shear rate. The simplest model that describes the shear thinning aspect is a 'power law' given by [100,101]:

$$\eta_v = K_v \gamma^{\cdot m} \quad (1.4)$$

where $K$ is a constant and $m$ is the power law index [102]. For a Newtonian fluid, the power law index $m$=1, whereas, for $m > 1$ and $m < 1$ it represents a shear thickening (dilatant) and a shear thinning (pseudoplastic) fluid, respectively. In general, many polymer solutions display the power law index $n$ value in the range 0.3 -0.7 [101]. Normally, smaller the value of the power law index, more shear thinning is expected in fluids [101, 103].

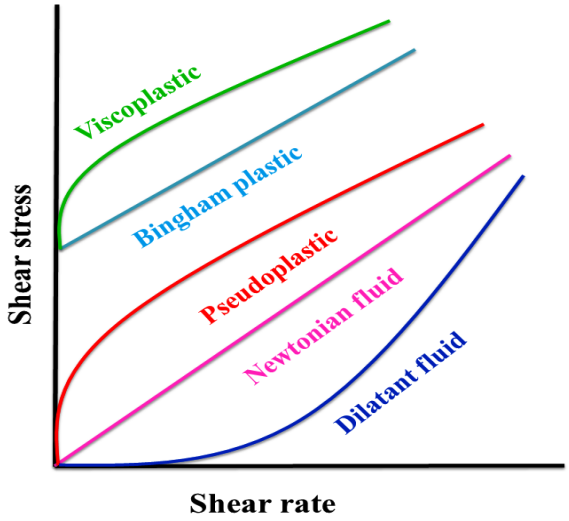


Figure 1.9: Flow curves of Newtonian and non- Newtonian fluids [104]

The study of rheological properties of materials has drawn numerous interest people in amongst academia and industries [104,105]. Rheology has profound scope in the field of material science, soft matter physics, geophysics, physiology, human biology, polymeric science, chemical engineering, petroleum technology and pharmaceutics and so on. Rheological principle is an important concept in material science as it involves the production of industrially relevant subject such as, cement, paint, and chocolate which possess complex flow properties. To study the flow behavior of liquids it is very much important for pharmaceutical industry to maintain the quality and integrity desired of the product.

Furthermore, rheology aspect becomes more interesting when subjected to a magnetic field. Magneto-rheological (MR) fluids are composed of magnetic particles, suspended in a carrier liquid. In a magnetic fluid, particles are in the range of 5-10 nm, while in MR fluid it can be few micron size limits. Upon application of magnetic field, the viscosity of MR fluid increases due to dipole-dipole interaction among the magnetic particles and chain like structure is formed in the direction of the magnetic field [106]. The dipole moment of a magnetic particle is given by [106]

$$\mu = V\chi H \qquad (1.5)$$

where $V = \frac{\Pi d^3}{6}$ is the volume of the particle, ($d$ is the diameter) is the magnetic susceptibility and $H$ is the applied magnetic field. The formation of chain-like structures leads to obstruction to the free flow of fluid, and consequently results in an increased viscosity [106]. The Brownian dispersion versus induced aggregation can be expressed by a coupling coefficient given by [106]:

$$\lambda = \frac{\Pi(\mu_0 \chi H)^2 d^3}{18 k_B T} \quad (1.6)$$

where $\mu_0$ , $H$, $k_B$ and $T$ are the permeability of the free space , the magnitude of the applied magnetic field, the Boltzmann constant and absolute temperature; respectively. When $\lambda \gg 1$, particle aggregation becomes extremely favorable in MR fluids. As for $\lambda \ll 1$, dispersion becomes extremely dominating. In presence of nanometric particles in a ferrofluid, the aggregation parameter is calculated by [106]

$$\lambda = \frac{\mu_0 M_s H \Pi d^3}{6 k_B T} \quad (1.7)$$

where $M_s$ is the saturation magnetization of the particles. The coupling parameter $\lambda$ is the key factor which determines the equilibrium suspension of the magnetic particles for chain-like structures.

When a magnetic field is applied to the MR fluids it displays fast, strong and reversible changes in their rheological responses [107, 108]. Consequently, they are very exciting for applications, such as, clutches, lubrication, damping devices, paints, pumps, anti-seismic elements etc. [109-111].

### 1.7: Biophysical perspectives of RE based nanosystems

Nanoscale materials have wide and far application in biomedical field. Many diagnostic and therapeutic techniques based on nanoscience and nanotechnologies are already in the clinical trial stages. Nanomedicine which link up with physical, chemical, biological and medical sciences, and the developments in nanomedicine have made it possible to investigate and treat biological systems at the cell and sub-cellular levels, thus providing

revolutionary approaches for the diagnosis, prevention and treatment of some fatal diseases, including cancer. In particular, nanoscale rare-earth oxide (REO) based materials have immense potential in the field of biomedical engineering as they are capable of offering quality optical imaging and as contrast agents for magnetic resonance imaging (MRI) and thus, have emerged as a vital asset in diagnostics and therapeutics [112,113]. Essentially, lanthanide materials have similar luminescence responses to that of semiconductor quantum dots (QDs) [114]. Nevertheless nanoscale REO systems enjoy a greater advantage over the QDs due to exhibition of a narrow emission line width, a higher emission intensity response and a higher photostability response [115]. All trivalent lanthanide ions, except $La^{3+}$ and $Lu^{3+}$ are known to possess unpaired electrons, and thus can exhibit paramagnetic behavior. Since Gd possess maximum number of unpaired electrons, it can offer highest magnetic moment. Therefore Gd containing compounds are regarded as idea contrast agents in medical diagnostics [116].

The increased of application of advanced nanomaterials in biomedical field has led to a great deal of finer studies wrt toxicity of the nanosystems [117]. Different researchers have assessed cytotoxicity aspect in different oxide systems, like $Gd_2O_3$ and $Dy_2O_3$ nanosystems [118, 119,120]. Moreover, nanoscale gadolinium hydroxide ($Gd(OH)_3$) has been exploited for its potential use in imaging and tracking of cells [121]. PEGylated mesoporous $Gd_2O_3$:$Eu^{3+}$ nanorods have also been examined which yielded noticeable cytotoxicity, insignificant hemolyticity, along with high biocompatibility and for deployment possibilities in disease diagnosis and chemotherapy [122]. Nanoceria having versatile oxidation states has also multi-enzyme properties, which can be promising in the field of bio-analysis, biomedicine, drug delivery and bioscaffolding [123].

### 1.8 Thesis objective and structure

The present work is a detailed investigation on nanometric $Gd_2O_3$ and $Gd_4O_3F_6$ powders both in pure and doped forms. Inclusion of other RE ions is also

considered to reveal selective *D-F* transitions in $Gd_2O_3$ and $Gd_4O_3F_6$ nanosystems. The effect of carbon ion irradiation on elongated $Gd_2O_3$ nanorods is investigated to exploit morphological evolution, optoelectronic responses and spin-spin relaxation features. Studies wrt physical and nano-bio interface of $Gd_2O_3$ nanoparticles and nanorods are also investigated. Furthermore, the magneto-rheological property of $Gd_2O_3$ nanorod based fluids is evaluated before and after γ-irradiation.

This thesis consists of seven chapters and a list of appendixes. An extensive literature survey as regards, growth of nanoscale material properties, luminescence, ion irradiation and overview of rheology can be addressed in the introductory part (*Chapter I*) of the thesis. For accessibility, the list of reference is provided at the end of each chapter.

The REO based nanosytems, pure and in doped forms are fabricated and their characterization through x-ray diffraction (XRD), transmission electron microscopy (TEM), Ultraviolet-Visible (UV-Vis) spectroscopy, photoluminescence (PL) spectroscopy, Raman spectroscopy and electron paramagnetic resonance (EPR) spectroscopy are discussed in *Chapter II*. Oriented attachment (OA) mediated characteristic growth of $Gd_2O_3$ nanorods obtained from nanoparticle seeds has been discussed.

The *Chapter III* deals with the manifestation and interconnected PL and EPR responses of the $Gd_2O_3$ nanorods subjected to 80 MeV carbon ion irradiation. The SHI induced shape evolution of the $Gd_2O_3$ nanorods has been also highlighted.

The *Chapter IV* focuses on the optical properties of the pure and RE ion doped $Gd_4O_3F_6$ nanosystems analyzed through optical absorption and photoluminescence (PL) spectroscopy studies. The effect of RE doping on the *D-F* transition mediated optical emission in RE oxyfluoride systems is discussed. Furthermore, intra *4f* transitions of $Eu^{3+}$ ions are recognized in the

host $Gd_4O_3F_6$ system. Alternatively, Judd-Ofelt (J-O) parameters of the $Eu^{3+}$ doped systems are ions calculated from the emission spectra.

In *Chapter V* the magneto-rheological properties of $Gd_2O_3$ based elongated structures are discussed with special emphasis on gamma irradiation.

The biophysical relevance of $Gd_2O_3$ nanoparticle and nanorod based systems has been discussed in *Chapter VI.*

Lastly, *chapter VII* highlights important conclusions drawn from the present investigation. The future scope of the present investigation is also summarized in this chapter.

**References**

[1] Goddard III, W. A., Brenner, D., Lyshevski, S. E., and Iafrate, G. J. *Handbook of Nanoscience, Engineering, and Technology*. 2nd ed., CRC Press, Florida, 2007.

[2] Tyner, K.M., Wokovich, A.M., Doub, W.H., Buhse, L.F., Sung, L.P., Watson, S.S., and Sadrieh, N. Comparing methods for detecting and characterizing metal oxide nanoparticles in unmodified commercial sunscreens. *Nanomedicine,* **4**:145–159, 2009.

[3]Fernando, R. H., and Sung, L. P. In Nanotechnology applications in coatings. *ACS Symposium Series; American Chemical Society*, Washington, DC, 2009.

[4] Fujishima, A., Rao, T. N., and Tryk, D.A. $TiO_2$ photocatalysts and diamond electrodes. *Electrochimica Acta,* 45: 4683-4690, 2000.

[5] Sun, Y., Wu, Q., and Shi, G. Graphene based new energy materials. *Energy and Environmental Science,* 4: 1113-1132, 2011.

[6] Zhang, L.L., Zhou, R., and Zhao X. S. Graphene-based materials as supercapacitor electrodes. *Journal of Materials Chemistry*, 20:5983-5992, 2010.

[7] Vivekchand, S. R. C., Rout, C. S., Subrahmanyam, K. S., Govindaraj, A., and Rao, C. N. R. Graphene-based electrochemical supercapacitors. *Journal of Chemical Sciences*, 120: 9-13, 2008.

[8] Subrahmanyam, K.S., Vivekchand, S. R. C., Govindaraj A., and Rao, C. N. R. A study of graphenes prepared by different methods: characterization, properties and solubilization. *Journal of Materials Chemistry*, 18: 1517-1523, 2008.

[9] Haque, N., Khalel, R, R., Parvez, N., Yadav, S., Hwisa, N., Al-Sharif, M. S., Awen, B. Z., and Molvi, K. Nanotechnology in cancer therapy: A review. *Journal of Chemical and Pharmaceutical Research*, 2: 161-168, 2010.

[10]Hsieh C.H, Chang M.T, Chien Y.J, Chou L.J, Chen L.J, and Chen C.D. Coaxial metal-oxide-semiconductor (MOS) Au/$Ga_2O_3$/GaN nanowires. *Nano Letters*, 8: 3288-3292, 2008.

[11] Bünzli J. C. G., and Choppin, G. R. *Lanthanide probes in life, chemical and earth sciences. Theory and practice.* Elsevier, Amsterdam,1989.

[12] Mornet, S., Vasseur, S., Grasset, F., and Duguet, E. Magnetic nanoparticle design for medical diagnosis and therapy. *Journal of Materials Chemistry*, 14: 2161-2175, 2004.

[13] Lee, M. H., Oh, S. G., Yi, S. C., Seo, D. S., Hong, J. P., Kim, C. O., Yoo, Y.K., and Yoo, J. S. Characterization of Eu-Doped $Y_2O_3$ Nanoparticles Prepared in Nonionic Reverse Microemulsions in Relation to Their Application for Field Emission Display. *Journal of the Electrochemical Society*, 147: 3139-3142, 2000.

[14] Ronda, C.R., Justel, T., and Niko, H. Rare earth phosphors: fundamentals and applications. *Journal of Alloys and Compounds,* 275–277: 669–676,1998.

[15] Foex, M., and Traverse, J.P. Investigations about crystalline transformation in rare earths sesquioxides at high temperatures. *Revue International des Hautes Temeratureset des Refractaires*, **3** :429-453, 1966.

[16] Zinkevich, M. Thermodynamics of rare earth sesquioxides. *Progress in Materials Science,* 52 **:** 597 -647, 2007.

[17] Gschneidner, K. A., Jr. and Eyring, L. *Handbook on the Physics and Chemistry of Rare Earths*, Elsevier, North Holland, Amsterdam, 1979.

[18] Salata, O. V. Applications of nanoparticles in biology and medicine. *Journal of Nanobiotechnology*, 2: 1-6, 2004.

[19] Gupta, A. K., and Gupta, M. Synthesis and surface engineering of iron oxide nanoparticles for biomedical applications. *Biomaterials,* 26: 3995-4021, 2005.

[20] Nishiura, M., and Hou, Z. Novel polymerization catalysts and hydride clusters from rare-earth metal dialkyls. *Nature Chemistry,* 2: 257–268, 2011.

[21] Devaraju, M.K., Yin, S., Sato, and T. A rapid hydrothermal synthesis of rare earth oxide activated $Y(OH)_3$ and $Y_2O_3$ nanotubes. *Nanotechnology,* 20: 305302(7p), 2009.

[22] Luo, N., Yang, C., Tian, X., Xiao, J., Liu, J., Chen, F., Zhang, D., Xu, D., Zhang, Y., Yang, G., Chen, D., and Li, Li. A general top-down approach to synthesize rare earth doped-$Gd_2O_3$ nanocrystals as dualmodal contrast agents. *Journal of Materials Chemistry B*, 2: 5891, 2014.

[23] Dhananjaya, N., Nagabhushana, H., Sharma, S.C., Rudraswamy, B., Shivakumara, C., and Nagabhushana, B.M. Hydrothermal synthesis of $Gd_2O_3$:$Eu^{3+}$ nanophosphors: Effect of surfactant on structural and luminescence properties. *Journal of Alloys and Compounds,* 587: 755-762, 2014.

[24] Tamrakar, R.K., Bisen, D. P., and Brahme, N. Combustion synthesis and upconversion luminescence properties of $Er^{3+}$, $Yb^{3+}$ doped gadolinium oxide nanophosphors. *Recent Research in Science and Technology*, 4: 70-72, 2012.

[25] Xinyu, Y.E., Wengui, G, Libin, X., Huaping, N., and Weidong, Z. A modified solution combustion method to superfine $Gd_2O_3$:$Eu^{3+}$ phosphor: preparation, phase transformation and optical properties. *Journal of Rare Earths,* 28: 345-350, 2010.

[26] Patra, A., Sominska, E., Ramesh, S., Koltypin, Yu., Zhong, Z., Minti, H., Reisfeld, R. and Gedanken, A. Sonochemical Preparation and Characterization of $Eu_2O_3$ and $Tb_2O_3$ Doped in and Coatedon Silica and Alumina Nanoparticles. *The Journal of Physical Chemistry B,* 103: 3361-3365, 1999.

[27] Niasari, M. S., Hosseinzadeh, G., and Davar, F. Synthesis of lanthanum hydroxide and lanthanum oxide nanoparticles by sonochemical method. *Journal of Alloys and Compounds,* 509: 4098–4103, 2011.

[28] Das, G.K., and Tan, T.T.Y. Rare-Earth-Doped and Codoped $Y_2O_3$ Nanomaterials as Potential Bioimaging Probes. *The Journal of Physical Chemistry C*, 112: 11211–11217, 2008.

[29] Sun, L., Yao, J., Liu, C., Liao, C., and Yan. C. Rare earth activated nanosized oxide phosphors: synthesis and optical properties. *Journal of Luminescence*, 87–89: 447-450, 2000.

[30] Pan, M., Meng, G.Y., Xin, H.W., Chen, C.S., Peng, D.K., and Lin Y.S. Pure and doped $CeO_2$ thin films prepared by MOCVD process. *Thin Solid Films*, 324: 89-93, 1998.

[31] Song, H.Z., Wang, H.B, Zha, S.W., Peng, D.K, and Meng, G.Y. Aerosol-assisted MOCVD growth of $Gd_2O_3$-doped $CeO_2$ thin SOFC electrolyte film on anode substrate. *Solid State Ionic*,156 : 249–254, 2003.

[32] Nguyen, T.D., and Do, T.O. General Two-Phase Routes to Synthesize Colloidal Metal Oxide Nanocrystals: Simple Synthesis and Ordered Self-Assembly Structures, *The Journal of Physical Chemistry C*, 113:11204–11214, 2009.

[33] Wang, T., Zhou, Ji., Shi, S., Li, Bo., and Zong, R. Preparation of size-controlled nanocrystalline infrared-to-visible upconverting phosphors $Gd_2O_3$: Yb, Er by using a water-in-oil microemulsion system. *Journal of Electroceramics*, 21: 765–769, 2008.

[34] Paek , J., Lee, C. H., Choi, J., Choi, S.Y., Kim, A., Lee, J. W., and Lee, K. Gadolinium Oxide Nanoring and Nanoplate: Anisotropic Shape Control. *Crystal Growth and Design,* 7 : 1378-1380, 2007.

[35] Gnanam, S., and Rajendran, V. Influence of Various Surfactants on Size, Morphology, and Optical Properties of $CeO_2$ Nanostructures via Facile Hydrothermal Route. *Journal of Nanoparticles*, 2013: 839391(6), 2013.

[36] Skandan, G., Hahn , H., and Parker, J.C. Nano-structured $Y_2O_3$: synthesis and relation to microstructure and properties. *Scripta Metallurgica et Materialia*, 25:2389- 2393, 1991.

[37] Du, G., and Tendeloo, G. V. Preparation and structure analysis of $Gd(OH)_3$ nanorods. *Nanotechnology*, 16: 595-597, 2005.

[38] Cao, Y.C. Synthesis of Square Gadolinium-Oxide Nanoplates, *Journal of the American Chemical Society,* 126:7456-7457, 2004.

[39] Si, R., Rui Si, Zhang, Y.W., You, L.P., and Yan, C.H. Rare-Earth Oxide Nanopolyhedra, Nanoplates, and Nanodisks. *Angewandte Chemie International Edition,* 44: 3256-3260, 2005.

[40] Yada, M., Mihara, M., Mouri, S., Kuroki, M., and Kijima, T. Rare Earth (Er, Tm, Yb, Lu) Oxide Nanotubes Templated by Dodecylsulfate Assemblies, *Advanced Materials,* 14:309-313, 2002.

[41] Das, G. K., Heng, B. C., Ng, S.C., White, T., Loo, J. S. C., D'Silva, L., Padmanabhan, P., Bhakoo, K. K., Selvan, S. T., and Tan, T. T. Y. Gadolinium Oxide Ultranarrow Nanorods as Multimodal Contrast Agents for Optical and Magnetic Resonance Imaging. *Langmuir,* 26: 8959–8965, 2010.

[42] Xu ,A.W., Fang, Y.P., You, L. P., and Liu, H.Q. et al. A Simple Method to Synthesize $Dy(OH)_3$ and $Dy_2O_3$ Nanotubes. *Journal of the American Chemical Society,* 125: 1494-1495, 2003.

[43] Raju, G. S. R., Pavitra, E., and Yu, J. S. Facile template free synthesis of $Gd_2O(CO_3)_2 \cdot H_2O$ chrysanthemum-like nanoflowers and luminescence properties of corresponding $Gd_2O_3$:$RE^{3+}$ spheres. *Dalton Transactions,* 42:11400-114010, 2013.

[44] Wang, Y., Liu, T., Wang, X., and Song, H. Controlled synthesis of ytterbium ion and erbium ion codoped gadolinium oxyfluoride hollow nanosphere with upconversion luminescence property. *Journal of Materials Research*, 28:848-855, 2013.

[45] Armelao, L., Bottaro, G., Bovo, L., Maccato, C., Pascolini, M., Sada, C., Soini, E., and Tondello, E. Luminescent properties of Eu doped Lanthanum oxyfluoride sol-gel thin films. *The Journal of Physical Chemistry C,* 113: 14429-14434, 2009.

[46] Huang, C.C., Liu, T.Y., Su, C.H., Lo, Y.W., Chen, J.H., and Yeh, C.S. Superparamagnetic hollow and paramagnetic porous $Gd_2O_3$ particles. *Chemistry of Materials,* 20: 3840-3848, 2008.

[47] Du, Y.P., Zhang, Y.W., Yan, Z.G., Sun, L.D., and Yan, C.H. Highly luminescent self-organized sub-2-nm EuOF nanowires. *Journal of the American Chemical Society,* 131: 16364-16365, 2009.

[48]Fujihara, S., Koji, S., and Kimura, T. Structure and optical properties of (Gd, Eu)$F_3$-nanocrystallized sol–gel silica films. *Journal of Materials Chemistry,* 14:1331-1335, 2004.

[49] Fujihara, S., and Tokumo, K. Chemical processing for inorganic fluoride and oxyfluoride materials having optical functions. *Journal of Fluorine Chemistry*, 130: 1106-11010, 2009.

[50] Antic-Fidanceva, E., Hölsä, J., Krupa, J.C., and Lastusaari, M. Crystal fields in ROF: $Tb^{3+}$ (R= La, Gd). *Journal of Alloys and Compounds,* 380: 303-309, 2004.

[51] Zachariasen, W. H. crystal chemical studies of the 5*f*-series of elements.XIV. oxyfluorides XOF. *Acta Crystallographica,* 4:231–236, 1951.

[52] Grzyb, T., Wiglusz, R. J., Nagirnyi, V., Kotlov, A., and Lis, S. Revised crystal structure and luminescent properties of gadolinium oxyfluoride $Gd_4O_3F_6$ doped with $Eu^{3+}$ ions. *Dalton Transactions,* 43: 6925-6934, 2014.

[53] Müller, J., and Petzel, T. High-temperature X-ray diffraction study of the rhombohedral-cubic phase transition of ROF with R=Y, La, Pr, Nd, Sm, Er. *Journal of Alloys and Compounds,* 224: 18–21, 1995.

[54]Fergus, J. W. Crystal structure of lanthanum oxyfluorides. J*ournal of Materials Science Letters,* 16: 267–269, 1997.

[55] Hölsä, J. Effect of non-stoichiometry on luminesce properties of lanthanum oxyfluorides. *Acta Chemica Scandinavica,* 45: 583–587, 1991.

[56] Li, R., Xiong, H., Liang, Y., Liu, Y., Zhang, N., and Gan, S. Rapid, morphology-controllable synthesis of GdOF:Ln3+ (Ln = Eu, Tb) crystals with multicolor-tunable luminescence properties. *New Journal of Chemistry,* 40:1792-1798, 2016.

[57] Grzyb,T., Węcławiak, M., and Lis, S. Influence of nanocrystals size on the structural and luminescent properties of GdOF:$Eu^{3+}$. *Journal of Alloys and Compounds,* 539: 82–89, 2012.

[58] Park, J,C., Moon, H,K., Kim, D.K., Byeon, S. H., Kim, B. C., and Suh, K.S. Morphology and cathodoluminescence of Li-doped $Gd_2O_3$:$Eu^{3+}$, a red phosphor operating at low voltages. *Applied Physics Letters,* 77: 2162-2164, 2000.

[59] Kang, Y. C., Park, S.B., Lenggoro, I.W., and Okuyama, K. $Gd_2O_3$:Eu phosphor particles with sphericity, submicron size and non-aggregation characteristics. *Journal of Physics and Chemistry of Solids*, 60:379–384,1999.

[60] Mercier, B., Dujardin, C., Ledoux, G., Louis, C., Tillement, O., and Perriat, P. Observation of the gap blueshift on $Gd_2O_3$: $Eu^{3+}$ nanoparticles. *Journal of Applied Physics,* 96: 650-653, 2004.

[61] Gordon,W O., Carter, J.A., and Tissue, B.M. Long-lifetime luminescence of lanthanide-doped gadolinium oxide nanoparticles for immunoassays. *Journal of Luminescence*, 108: 339-342, 2004.

[62] Bedekar, V., Dutta, D. P., Mohapatra, M., Godbole, S. V., Ghildiyal, R., and Tyagi, A. K. Rare-earth doped gadolinia based phosphors for potential multicolor and white light emitting deep UV LEDs. *Nanotechnology,* 20: 125707 (9pp), 2009.

[63] Prokofiev, A V., Shelykh, A.I., and Melekh, B.T. Periodicity in the band gap variation of $Ln_2X_3$ (X = O, S, Se) in the lanthanide series. *Journal of Alloys and Compounds,* 242: 41-44, 1996.

[64] Rozhkov, V.A., Trusova, A.Y., and Berezhnoy, I.G. Silicon MIS structures using samarium oxide films. *Thin Solid Films,* 325:151–155, 1998.

[65] Rao, G. V.S., Ramdas, S., Mehrotra, P.N., and Rao, C.N.R. Electrical Transport in Rare-Earth Oxides. *Journal of Solid State Chemistry,* 2: 377-384, 1970.

[66] Guo, H., Dong, N., Yin, M., Zhang, W., Lou, L., and Xia, S. Visible Upconversion in Rare Earth Ion-Doped $Gd_2O_3$ Nanocrystals. *The Journal of Physical Chemistry B*, 108: 19205-19209, 2004.

[67] Gibart, P., Auzel, F., Guillaume, J.C., and Zahraman, K. Below band-gap IR response of substrate-free GaAs solar cells using two-photon up-conversion. *Japanese Journal of Applied Physics*, 35 : 4401-4402, 1996.

[68] Sivakumar, S., Veggel, F.C. J. M. V., and Raudsepp, M. Bright White Light through Up-Conversion of a Single NIR Source from Sol−Gel-Derived Thin Film Made with $Ln^{3+}$ -Doped $LaF_3$ Nanoparticles. *Journal of the American Chemical,* 127: 12464–12465, 2005.

[69] Hölsä, J., Piriou, B., and Räsänen, M. IR- and Raman-active normal vibrations of rare earth oxyiluorides, REOF; RE=Y, La, and Gd. *Spectrochimica Acta Part A: Molecular Spectroscopy*, 49: 465–470, 1993.

[70] Grzyb, T., and Lis, S. Structural and Spectroscopic Properties of LaOF:$Eu^{3+}$ Nanocrystals Prepared by the Sol Gel Pechini Method. *Inorganic Chemistry,* 50: 8112–8120, 2011.

[71] Du, Y.-P., Zhang, Y. W., Sun, L. D., and Yan, C.H. Luminescent Monodisperse Nanocrystals of Lanthanide Oxyfluorides Synthesized from Trifluoroacetate Precursors in High-Boiling Solvents. *The Journal of Physical Chemistry C,* 112: 405–415, 2008.

[72] Rakov, N., Barbosa, J. de A.B., Guimarães, R.B., and Maciel, G. S. Spectroscopic properties of $Eu^{3+}$- and $Eu^{3+}$:$Yb^{3+}$ -doped LaOF crystalline powders prepared by combustion synthesis. *Journal of Alloys and Compounds,* 534: 32–36,2012 .

[73] Gao, D., Zheng, H., Zhang, X., Fu, Z., Zhang, Z., Tian, Y., and Cui, M. Efficient fluorescence emission and photon conversion of LaOF : $Eu^{3+}$ nanocrystals. *Applied Physics Letters,* 98: 011907-3, 2011.

[74] Zhang, X., Gao, D., and Li, L. Down- and up-conversion luminescence of $Tm^{3+}$ / $Ho^{3+}$ codoped LaOF nanoparticles. *Journal of Applied Physics,* 107:123528-5, 2010.

[75] Shang, M., Li, G., Kang, X., Yang, D., Geng, D., Peng, C., Cheng, Z., Lian, H., and Lin, J. LaOF : Eu3+ nanocrystals: hydrothermal synthesis, white and color-tuning emission properties. *Dalton Transactions,* 41: 5571– 5580, 2012.

[76] Shang, M., Geng, D., Kang, X., Yang, D., Zhang, Y., and Lin, J. Hydrothermal Derived LaOF:$Ln^{3+}$ (Ln = Eu, Tb, Sm, Dy, Tm, and/or Ho) Nanocrystals with Multicolor-Tunable Emission Properties. *Inorganic Chemistry,* **51**, 11106–11116, 2012.

[77] Passuello, T., Piccinelli, F., Pedroni, M., Bettinelli, M., Mangiarini, F., Naccache, R., Vetrone, F., Capobianco, J.A., and Speghini, A. White light upconversion of nanocrystalline Er/Tm/Yb doped tetragonal $Gd_4O_3F_6$. *Optical Materials,* 33:643–646, 2011.

[78] Passuello, T., Piccinelli, F., Pedroni, M., Polizzi , S., Mangiarini , F., Vetrone, F., Bettinelli, M., Speghini, A. NIR-to-visible and NIR-to-NIR upconversion in lanthanide doped nanocrystalline GdOF with trigonal structure. *Optical Materials,* 33:1500–1505, 2011.

[79] Williams, J. S. Materials modification with ion beams, *Reports on Progress in Physics*. 49: 491-587, 1986.

[80] Lindhard, J., and Schad, M. Energy dissipation by ions in the keV region. *Physical Review,* **124**, 128-130, 1961.

[81]Mehta, G.K. Materials modification with high energy heavy ions. *Nuclear Instruments and Methods in Physics Research Section A: Accelerators, Spectrometers, Detectors and Associated Equipment*, 382: 335-342, 1996.

[82] Swanson, M. L., Parsons, J.R., and Hoelke, C.W. Damaged regions in neutron-irradiated and ion-bombarded Ge and Si. *Radiation Effects,* 9: 249-256, 1971.

[83] Hensel, H., and Urbassek, H. M. Implantation and damage under low-energy Si self-bombardment. *Physical Review B,* 57: 4756-4763, 1998.

[84] Fleischer, R. L., Price, P. B., and Walker, R. M. Ion explosion spike mechanism for formation of charged-particle tracks in solids. *Journal of Applied Physics,* 36:3645-3652, 1965.

[85] Toulemonde, M., Dufour, C., and Paumier, E. Transient thermal process after a high-energy heavy-ion irradiation of amorphous metals and semiconductors. *Physical Review B,* 46: 14362-14369, 1992.

[86] Dufour, C., Audouard, A., Beuneu, F., Dural, J., Girard, J.P., Hairie, A., Levalois, M., Paumier, E., and Toulemonde , M. A high-resistivity phase induced by swift heavy-ion irradiation of Bi: a probe for thermal spike damage. *Journal of Physics: Condensed Matter,* 5: 4573-4584, 1993.

[87] Norman, A. Thermal spike effects in heavy-ion tracks. *Radiation Research Supplement,* 7: 33-37, 1967.

[88] Brown, R. A., and Williams, J. S. Crystalline-to-amorphous phase transformation in ion-irradiated GaAs. *Physical Review B*, 64: 155202 (1-6), 2001.

[89] Benyagoub, A. Mechanism of the monoclinic-to-tetragonal phase transition induced in zirconia and hafnia by swift heavy ions *Physical Review B,* 72: 094114-6 ,2005.

[90] Benyagoub, A., Levesque, F., Couvreur, F., Mougel, C. G., Dufour, C., and Paumier, E. Evidence of a phase transition induced in zirconia by high energy heavy ions. *Applied Physics Letters,* 77: 3197-3199, 2000.

[91] Bayan, S., and Mohanta, D. Effect of 80-MeV nitrogen ion irradiation on ZnO nanoparticles: Mechanism of selective defect related radiative emission features. *Nuclear Instruments and Methods in Physics Research Section B: Beam Interactions with Materials and Atoms*, 269: 374-379, 2011.

[92] Bayan, S., and Mohanta, D. Fragmentation of elongated-shaped ZnO nanostructures into spherical particles by swift ion impact. *Physica E,* 54: 288-294, 2013.

[93] Mishra, Y.K., Avasthi, D.K., Kulriya, P.K., Singh, F., Kabiraj, D., Tripathi, A., Pivin, J.C., Bayer, I.S., and Biswas, A. Controlled growth of gold

nanoparticles induced by ion irradiation: An in situ x-ray diffraction study. *Applield Physics Letters,* 90: 073110-3, 2007.

[94] Mohanta, D., Ahmed, G.A., Choudhury, A., Singh, F., Avasthi, D.K., Boyer, G., and Stanciu, G.A. Scanning probe microscopy, luminescence and third harmonic generation studies of elongated CdS:Mn nanostructures developed by energetic oxygen-ion-impact. *The European Physical Journal Applied Physics*, 35: 29-36,2006.

[95] Lian, J., Zhou, W., Wei, Q.M., Wang, L.M., Boatner, L.A., and Ewing, R.C. Simultaneous formation of surface ripples and metallic nanodots induced by phase decomposition and focused ion beam patterning. *Applied Physics Letters,* 88: 093112-3, 2006

[96] Tang, M., Lu, P., Valdez J.A., and Sickafus K.E. Ion-irradiation-induced phase transformation in rare earth sesquioxides ($Dy_2O_3$,$Er_2O_3$,$Lu_2O_3$). *Journal of Applied Physics*, 99: 063514-7, 2006.

[97] Tang, M., Valdez, J. A., Sickafus, K. E., and Lu, P. Order-disorder phase transformation in ion-irradiated rare earth sesquioxides. *Applied Physics Letters,* 90: 151907-3, 2007.

[98] Antic, B., Kremenovic, A., Draganic, I., Colomban, P., Radovic, D. V., Blanusa, J.,Tadic, M., and Mitric, M. Effects of $O^{2+}$ ions beam irradiation on crystal structure of rare earth sesquioxides. *Applied Surface Science,* 255: 7601-7604, 2009.

[99] Lesueur, D., and Dunlop, A.Damage creation via electronic excitations in metallic targets part II : A theoretical model. *Radiation Effects and Defects in Solids*, 126:163-172, 1993.

[100**]** Khan, S. A., Royer, J.R., and Raghavan, S.R. Rheology: Tools and Methods. *Aviation fuels with improved fire safety: A proceeding* ,31-46,1997.

[101] Chhabra ,R.P. *Rheolgy of complex fluids, part I*. Springer,Berlin, 3-34,2010.

[102] Mezger. T. G. *The Rheology Handbook: For Users of Rotational and Oscillatory Rheometers.* Vincentz Network GmbH&Co KG, 2006.

[103] Thirupathi, G., and Singh, R. Study of Magnetoviscosity of Ferromagnetic MnZn-Ferrite Ferrofluid. *IEEE Transactions on Magnetics*,51: 4600404, 2015.

[104] Park, B. J., Park, B. O., Ryu, B. H., Choi, Y. M., Kwon, K. S., and Choi, H. J. Rheological properties of Ag suspended fluid for inkjet printing. *Journal of Applied Physics,* 108: 102803-5, 2010.

[105] Giannelis, E.P. Polymer Layered Silicate Nanocomposites, *Advanced Materials,* 8: 29-35, 1996.

[106] Samouhos, S., and McKinley, G. Carbon Nanotube–Magnetite Composites, With Applications to Developing Unique Magnetorheological Fluids. *Journal of Fluids Engineering,* 129: 429-437, 2007.

[107] Claracq, J., Sarrazin, J., and Montfort, J.P. Viscoelastic properties of magnetorheological fluids. *Rheologica Acta*, 43: 38–49, 2004.

[108] de Vicente, J., Klingenberg, D.J., and Alvarez, R. H. Magnetorheological fluids: a review. *Soft Matter*, 7 :3701–10, 2011.

[109] Powell, L. A., Hu, W., and Wereley, N. M. Magnetorheological fluid composites synthesized for helicopter landing gear applications. *Journal of Intelligent Material Systems and Structures,* 24: 1043–1048, 2013.

[110] Park, B. J., Fang, F. F., and Choi, H. J. Magnetorheology: materials and application. *Soft Matter,* 6: 5246–5253, 2010.

[111] Jolly, M. R., Bender, J. W., and Carlson, J. D. Properties and applications of commercial magnetorheological fluids. *Journal of Intelligent Material Systems and Structures,* 10: 5–13, 1999.

[112] Bridot, J.L., Faure, A.C., Laurent, S., Riviére, C., Billotey, C., Hiba, B., Janier, M., Josserand, V., Coll, J.L., Elst, L. V., Muller, R., Roux, S., Perriat, P., and Tillement, O. Hybrid Gadolinium Oxide Nanoparticles: Multimodal

Contrast Agents for in Vivo Imaging. *Journal of the American Chemical Society*, 129: 5076-5084, 2007.

[113]Petoral, J. R.M., Söderlind, F., Klasson, A., Suska, A., Fortin, M.A., Abrikossova, N., Selegård, L., Käll, P.O., Engström, M., and Uvdal, K. Synthesis and characterization of $Tb^{3+}$-doped $Gd_2O_3$ nanocrystals: A bifunctional material with combined fluorescent labeling and MRI contrast agent properties. *The Journal of Physical Chemistry C,* 113: 6913 -6920, 2009.

[114] Riegler, J., and Nann, T. Application of luminescent nanocrystals as labels for biological molecules. *Analytical and Bioanalytical Chemistry*, 379: 913-919, 2004.

[115] Torsello, G. Lomascolo, M., Licciulli, A., Diso, D., Tundo S., and Mazzer, M. The origin of highly efficient selective emission in rare-earth oxides for thermophotovoltaic applications. *Nature Materials* 3: 632-637, 2004.

[116] Park, J. Y., Baek, M. J., Choi, E. S, Woo, S., Kim, J. H., Kim,T. J., Jung, J. C., Chae, K. S., Chang, Y., and Lee, G. H. Paramagnetic ultrasmall gadolinium oxide nanoparticles as advanced T1 MRI contrast agent: Account for large longitudinal relaxivity, optimal particle diameter, and in vivo T1 MR images. *ACS Nano* 3: 3663-3669, 2009.

[117] Soto, K., Garza, K.M., and Murr L.E. Cytotoxic effects of aggregated nanomaterials. *Acta Biomaterialia* 3: 351–358, 2007.

[118] Heinrich, M. C., Kuhlmann, M. K., Kohlbacher, S., Scheer, M., Grgic, A., Heckmann, M. B., and Uder, M. Cytotoxicity of Iodinated and Gadolinium-based Contrast Agents in Renal Tubular Cells at Angiographic Concentrations: In Vitro Study. *Radiology,* 242: 425–434, 2007.

[119] Das,G. K., Zhang, Y., D'Silva, L., Padmanabhan, P., Heng, B. C., Loo, J. S. C., Selvan, S. T., Bhakoo,K. K., and Tan, T. T. Y. Single-phase $Dy_2O_3$:$Tb^{3+}$ nanocrystals as dual-modal contrast agent for high field magnetic resonance and optical Imaging. *Chemistry of Materials,* 23: 2439–2446, 2011.

[120] Bouzigues, C., Gacoin, T., and Alexandrou, A. Biological Applications of Rare-Earth Based Nanoparticles. *ACS Nano*, 5:8488-8505, 2011.

[121] Hemmer, E., Kohl, Y., Colquhoun, V., Thielecke, H., Soga, K., and Mathur, S. Probing Cytotoxicity of Gadolinium Hydroxide Nanostructures.*The Journal of Physical Chemistry B,* 114: 4358–4365, 2010.

[122] Liu, Z., Liu, X., Yuan, Q., Dong, K., Jiang, L., Li, Z., Ren, J., and Qu, X. Hybrid mesoporous gadolinium oxide nanorods: a platform for multimodal imaging and enhanced insoluble anticancer drug delivery with low systemic toxicity. *Journal of Materials Chemistry,* 22:14982-14990, 2012.

[123] Xu, C., and Qu, X. Cerium oxide nanoparticle: a remarkably versatile rare earth nanomaterial for biological applications. *NPG Asia Materials,* 6:1-16, 2014.